

# CrystEngComm

Accepted Manuscript



This is an *Accepted Manuscript*, which has been through the Royal Society of Chemistry peer review process and has been accepted for publication.

*Accepted Manuscripts* are published online shortly after acceptance, before technical editing, formatting and proof reading. Using this free service, authors can make their results available to the community, in citable form, before we publish the edited article. We will replace this *Accepted Manuscript* with the edited and formatted *Advance Article* as soon as it is available.

You can find more information about *Accepted Manuscripts* in the [Information for Authors](#).

Please note that technical editing may introduce minor changes to the text and/or graphics, which may alter content. The journal's standard [Terms & Conditions](#) and the [Ethical guidelines](#) still apply. In no event shall the Royal Society of Chemistry be held responsible for any errors or omissions in this *Accepted Manuscript* or any consequences arising from the use of any information it contains.

Cite this: DOI: 10.1039/c0xx00000x

www.rsc.org/xxxxxx

ARTICLE TYPE

# Preparation, Optical Property and Field-effect Mobility Investigation of Stable White-emissive Doped Organic Crystal

Huan Wang,<sup>\*a</sup> Yang Zhao,<sup>a</sup> Zengqi Xie,<sup>b</sup> Hui Shang,<sup>\*c</sup> Huaiyuan Wang,<sup>a</sup> Feng Li<sup>d</sup> and Yuguang Ma<sup>\*b</sup>

Received (in XXX, XXX) Xth XXXXXXXXX 20XX, Accepted Xth XXXXXXXXX 20XX

DOI: 10.1039/b000000x

Different with most of reported white-light-emission amorphous doped organic films through precisely controlling a very low and specific doping concentration usually smaller than 1%, the tetracene (Tc) and pentacene (Pc) doubly doped *trans*-1,4-distyrylbenzene (DSB) crystal (DSB<Tc-Pc) prepared by physical vapor transport (PVT) method could present a white-light emission with approximately 10% dopant mol concentrations (DSB: Tc: Pc = 20: 1: 0.9), attributed to the intermolecular strong arene-arene interactions inducing the cross donor-acceptor transition dipole arrangement that is efficient to restrict energy transfer. Then the time-resolved fluorescence properties have been detailedly discussed to analyze the energy transfer process between DSB and Tc/Pc molecules in the DSB<Tc-Pc crystal. Simultaneously, the structural ordering maintenance of the white-emissive doped crystal has been verified by atomic force microscopy (AFM) and X-ray diffraction (XRD), which benefits for the carrier transport; and the hole and electron field-effect mobility was measured with  $1.62 \times 10^{-2} \text{ cm}^2/\text{Vs}$  and  $2.15 \times 10^{-4} \text{ cm}^2/\text{Vs}$ , respectively. Also due to the intermolecular highly ordered arrangement, the DSB<Tc-Pc crystal can exhibit the ideal and stable white-light emission with the CIE coordinates approaching to (0.33, 0.33) even under the high pumping laser energy excitation. The primary results indicate the stable white-emissive doped organic crystal can be prepared by PVT and has the high potential of realizing a white electroluminescence based on the device configurations of light-emitting diodes or field-effect transistors.

## Introduction

Organic crystals constructed by  $\pi$ -conjugated molecules have attracted great attention in the field of organic optoelectronic materials,<sup>1-4</sup> of which the definite structures provide a model to investigate the relationship between molecular stacking modes and optoelectronic performance (luminescence and carrier mobility).<sup>5,6</sup> In the meanwhile, the superiorities of organic crystals such as high thermal stability and high carrier mobility make them attractive candidates for optoelectronic devices such as optically pumped lasers,<sup>7-9</sup> field-effect transistors,<sup>10-12</sup> electroluminescence,<sup>13-15</sup> and photovoltaic cell.<sup>16-18</sup> Doped organic molecular crystals have been paid much attention as early as 1970's and stimulated emissions in some systems were observed in succession.<sup>19,20</sup> Doping has the advantage for tuning the emission color and decreasing the absorption loss by using the energy transfer. For the white-emissive doped organic crystal growth, the host-guest system of two cyan-orange components or three blue-green-red components is usually considered. Yao and coworkers successfully fabricated the white luminescent nanowires by merely blending a blue dye with an orange one through the adsorbent-assisted physical vapor deposition (PVD) method.<sup>21</sup> Notably, micro- or nano-size organic crystals are lack of structural definition and limited the application in optoelectronic devices. Thus, large-size (millimeter scale)

crystals are high demand for the fabrication of devices, which can even endure the high current density up to several  $\text{kA}\cdot\text{cm}^{-2}$  without luminescence efficiency roll-off<sup>22,23</sup> and will open a realistic route towards organic bright lighting devices.

Recently, high-luminescence and large-size doped organic crystals with structural-order retention have been prepared by physical vapor transport (PVT) method based on *trans*-1,4-distyrylbenzene (DSB) as the host and tetracene (Tc) or pentacene (Pc) as the guest.<sup>24</sup> Tc doped DSB crystal (abbreviated as DSB<Tc crystal) and Pc doped DSB crystal (abbreviated as DSB<Pc crystal) present the green and red light emissions, respectively; and the doping concentrations of Tc or Pc molecules can approach to 8% which are mainly attributed to the structural comparability of host and guest molecules and their similar 'herringbone' type molecular stacking in crystals.<sup>25-27</sup> Subsequently, it has been demonstrated that so high doping concentration is due to the mutually perpendicular transition dipole orientations between host and guest, which results in a small value of orientation factor  $\kappa^2$  and thereby reduces the efficiency of resonance energy transfer (RET).<sup>28</sup> Because a cross dipole arrangement between the donor and acceptor molecules could be efficient to restrict energy transfer process and then to realize a partial energy transfer even at high doping concentrations, it will facilitate us to prepare a white-light emissive organic crystal overcoming the concentration-sensitivity problem and having good color reproducibility and stability.

In this paper, Tc and Pc as green and red dopants respectively, were simultaneously doped into the DSB crystal (abbreviated as DSB<Tc-Pc crystal) by PVT method. Combined with the crystal growth thermodynamic characteristics,<sup>29</sup> the white-emissive DSB<Tc-Pc crystal with a specific mol ratio of host to guest molecules (DSB: Tc: Pc = 20: 1: 0.9) has been obtained under the conditions of suitable temperature. The host DSB and the guest Tc/Pc are all linear and planar molecular configurations and their intermolecular strong arene-arene interactions induce the cross dipole arrangement between DSB and Tc/Pc in the doped crystal formation process which is inefficient for energy transfer, thus to realize the high doping concentrations (Tc and Pc added up to nearly 10%). The energy transfer occurring not only from the donor DSB to the acceptors Tc and Pc but also from the acceptor Tc to the acceptor Pc has been verified by time-resolved fluorescence. The DSB<Tc-Pc crystal maintains the structural ordering as proved by X-ray diffraction (XRD) and atomic force microscopy (AFM) analysis; and the crystal mobilities deduced from the field-effect transistor (FET) measurements for hole and electron are  $1.62 \times 10^{-2} \text{ cm}^2/\text{Vs}$  and  $2.15 \times 10^{-4} \text{ cm}^2/\text{Vs}$ , respectively, of which the hole mobility is comparable to that of pure DSB crystal. Based on the highly ordered arrangement between host-guest molecules, the white-emissive DSB<Tc-Pc crystal under the high pumping laser energy excitation still exhibits a good color stability with the Commission International del'Eclairage (CIE) coordinates approaching to an ideal white light (0.33, 0.33). The preliminary analyses on the optoelectronic properties of the white-emissive DSB<Tc-Pc crystal prepared by PVT will guide us to design and fabricate the stable organic white lighting crystal device.

## Experimental section

UV-vis absorption and fluorescence spectra were recorded using UV-3100 and RF-5301PC spectrophotometers, respectively. The atomic force microscope (AFM) images were recorded on a Seiko SPA 400 with an SPI 3800 probe station in tapping mode (dynamic force mode). Commercially available Si cantilevers with a force constant of 20 N/m were used. The wide-angle X-ray diffraction was detected with a Rigaku X-ray diffractometer (D/Max-rA, using Cu-K $\alpha$  radiation of wavelength 1.542 Å), and in the test the slice crystal was flatted parallel to the single-crystal Si substrate.

High performance liquid chromatography (LC-20A) was used to analyze the component content of the doped crystals. The C18 (octadecylsilyl, ODS) was used as the filling matters in column, and the column temperature was controlled as 40 °C in the test process. Ultraviolet detector (254nm) was in response to different component. The mixed solution of CH<sub>3</sub>OH (80%, vol.) and H<sub>2</sub>O (20%, vol.) were used as the flow phase and the flow rate was controlled as 1 mL/min. All the detected components could be solved in tetrahydrofuran (THF).

Time-resolved fluorescence measurements were performed by the time-correlated single photon counting (TCSPC) system under right-angle sample geometry. A 379 nm picosecond diode laser (Edinburgh Instruments EPL375, repetition rate 20MHz) were used to excite the sample. The emission was detected by a photomultiplier tube (Hamamatsu H5783p) and a TCSPC board (Becker&Hickel SPC-130). The instrument response function

(IRF) is about 220 ps. All the measurements were done at room temperature (22 °C).

For the pumping laser excitation test, the slice crystals adhered to the quartz substrate were irradiated by the third harmonic (355 nm) of a Nd:YAG (yttrium-aluminum-garnet) laser at a repetition rate of 10 Hz and pulse duration of about 10 ns. The energy of the pumping laser was adjusted by using the calibrated neutral density filters. The beam was focused into a stripe whose shape is adjusted to 4×0.5 mm through using a cylindrical lens and a slit. The edge emission of the crystals was detected using a charge-coupled-device (CCD) fiber spectrograph. All the measurements were carried out at room temperature under ambient conditions.

Crystal FET fabrications: A 200-nm-thick SiO<sub>2</sub> layer on a highly doped silicon wafer was used as an insulator. A 100-nm-thick poly(methylmethacrylate) (PMMA) layer was spin coated from a toluene solution (30 mg/mL) onto the wafer. After the PMMA deposition, the substrates were maintained overnight in an oven at 70 °C and were subsequently annealed at 100 °C for 3 h under a N<sub>2</sub> atmosphere. Next, the crystal was carefully placed on the substrate. The 200-nm-thick top-contact gold or calcium electrodes were thermally evaporated on the crystal surface at a rate of 0.1–0.2 nm/s through a shadow mask under a background pressure of  $1 \times 10^{-6}$  mbar. The channel length and width were checked with an optical microscope. The FET measurements were carried out using semiconductor parameter analyzer HP4155C (Agilent Technologies) in a glovebox without exposing the substrate to air.

Tetracene and pentacene, purchased from J&K ACROS (98%), were purified by sublimation few times before use. *Trans*-1,4-distyrylbenzene was synthesized and purified as referred to in our previous work.<sup>30</sup>

## Results and discussions

### 1. Preparation of the white-emissive DSB<Tc-Pc crystal

The energy transfer efficiency in a donor-acceptor system is strongly dependent on the transition dipole arrangement between the donor and acceptor molecules which can be described by the orientation factor  $\kappa^2$ , ranging from 0 to 4 (Figure 1a); for instance when the two dipoles are perpendicular one to another, that is the orientation factor  $\kappa^2$  equal to zero, the energy transfer process will be forbidden, as prediction of the theory developed by Förster more than 60 years ago.<sup>31</sup> DSB, a brick-like conjugated molecule with dipole transition along its long molecular direction as shown in Figure 1b, tends to form 'herringbone' type stacking in crystal and the crystal shows intensive blue emission with photoluminescence quantum efficiency as high as 70%.<sup>25,32</sup> Both Tc and Pc possess quite similar molecular configurations and also molecular stacking modes as that of DSB,<sup>26,33,34</sup> However, their dipole transition direction is totally different that is along the short molecular axes (Figure 1b).<sup>35,36</sup> Meanwhile, Tc and Pc show green and red emission in dilute solutions respectively; and their absorption spectra have some overlaps with DSB crystal emission spectrum shown in Figure 1c, which means the preparation of the white-emissive doped crystal with DSB as the energy donor and Tc/Pc as the energy acceptors is feasible. The spectra data are summarized in Table 1.

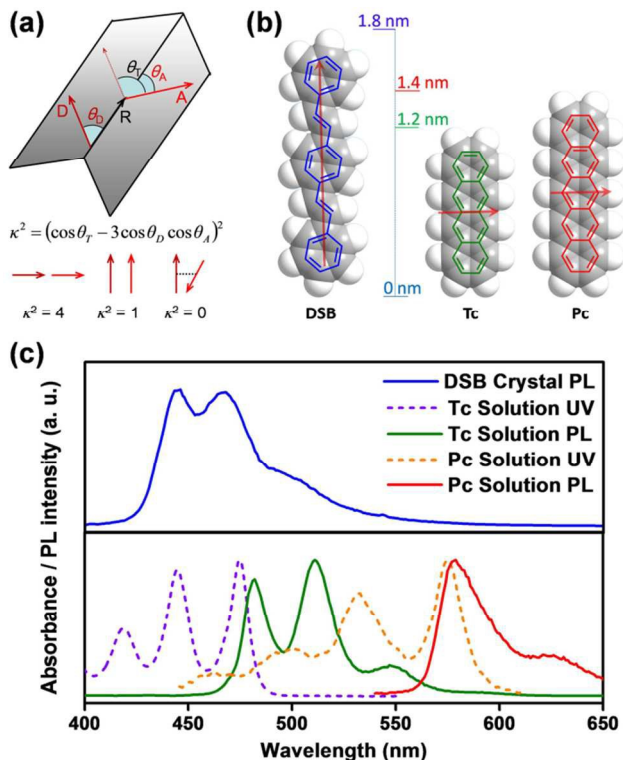


**Fig. 1** (a) Spatial orientation of donor and acceptor dipoles (red arrows) and the relationship with orientation factor  $\kappa^2$ .  $\kappa^2 = (\cos\theta_T - 3\cos\theta_D\cos\theta_A)^2$ , where  $\theta_D$  is the angle between the donor dipole and R (the vector from the donor to the acceptor).  $\theta_A$  is the angle between the acceptor dipole and R.  $\theta_T$  is the angle between donor and acceptor dipoles. (b) Molecular structures of DSB, Tc and Pc. The dipole transition direction of DSB is along its long molecular axis, while those of Tc and Pc are along their short axes. (c) The emission spectrum of the DSB crystal (upper). The absorption and emission spectra of the Tc and Pc solution with chloroform as the solvent (lower).

**Table 1** Summaries of the absorption and emission wavelengths of DSB crystal and Tc/ Pc solutions.

Materials	Absorption wavelength (nm)			Emission wavelength (nm)		
	0–2	0–1	0–0	0–0	0–1	0–2
DSB crystal	–	–	–	444	467	500
Tc solution	419	445	475	482	511	549
Pc solution	496	532	575	579	625	–

The crystal growth apparatus was reported in our previous work as shown in Figure 2a.<sup>37</sup> Pc, DSB and Tc were placed sequentially in the source zone of the apparatus where the temperature gradient varied from 250 °C to 150 °C according to the proper sublimation temperatures of the materials. The sublimated molecules were transported with a carrier gas (Ar, 99.999%), and then the crystals grew in the growth zone. After two or three days of stable growth, the large-size slice crystals emitting the white light under the excitation of ultraviolet light were formed hanging inside of the growth tube.

The emission spectrum of the white-emissive DSB<Tc-Pc crystal is shown in Figure 2b (Inserts are the corresponding

optical photographs of crystals under the ultraviolet lamp), where the 0-0/0-1 transition emissions of DSB, Tc and Pc are about 444/467 nm, 497/531 nm and 603/654 nm, respectively. The emission peaks of Tc and Pc in the DSB<Tc-Pc crystal have about 20–30 nm red shifts relative to those in the solution, which may be caused by the conjugated effect of Tc/Pc with the surrounding DSB molecules. Figure 2c shows the CIE coordinate of (0.36, 0.37) corresponding to the emission of above DSB<Tc-Pc crystal shown in Figure 2b, approaching to an ideal white light (0.33, 0.33); and the mol ratio of host to guest molecules (DSB: Tc: Pc = 20: 1: 0.9) was estimated by chromatograph analysis (see supporting information for the details).

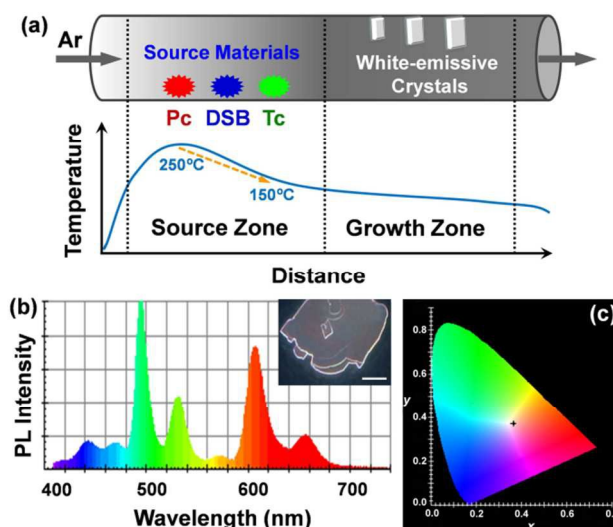


**Fig. 2** (a) Schematics of the apparatus for the growth of doped crystals by the physical vapor transport method. The temperature in the apparatus is controlled as shown in the bottom. The temperatures of Pc, DSB and Tc heated for the sublimation are controlled as 250 °C, 210 °C and 150 °C respectively in the source zone; and the white-emissive crystals could be obtained in the growth zone. (b) The emission spectrum of the DSB<Tc-Pc crystal (Inserts are the corresponding optical photographs of crystals under the ultraviolet lamp, and the scale bar is 1 millimeter). (c) CIE chromaticity diagram marked with the cross (0.36, 0.37) corresponding to the crystal emission shown in Figure 2b.

In the white-emissive doubly doped DSB<Tc-Pc crystal, the total dopant concentrations including both Tc and Pc up to approximately 10% are attributed to their similar linear and planar molecular configurations as well as that of DSB; but the energy transfer occurs partially from donor to acceptor as a result of their almost mutually perpendicular transition dipole arrangement, which will be closely followed by discussion.

## 2. Time-resolved fluorescence to analyze the energy transfer process

Figure 3a shows the photoluminescence decay curves of DSB<Tc crystals with two different mol ratios (DSB: Tc = 33: 1, 18: 1), and the white-emissive doubly doped DSB<Tc-Pc crystal (DSB: Tc: Pc = 20: 1: 0.9) monitored at the emission wavelength of 444 nm. The decay time of the donor DSB in above three doped crystals are 1.49 ns, 1.04 ns and 0.11 ns, respectively. Obviously, the decay time of DSB in the DSB<Tc-Pc crystal is much shorter than that in the DSB<Tc crystals although the mol ratio of DSB to Tc (20: 1) in the DSB<Tc-Pc crystal is in

between 33: 1 and 18: 1. That means the energy transfer occur not only from the donor DSB to the acceptor Tc but also from the donor DSB to the acceptor Pc in the white-emissive doubly doped crystal. As shown in Figure 3b, the photoluminescence decay curves of DSB<Tc crystals with two different mol ratios (DSB: Tc = 33: 1, 18: 1), and the white-emissive doubly doped DSB<Tc-Pc crystal (DSB: Tc: Pc = 20: 1: 0.9) monitored at the emission wavelength of 531 nm. The decay time of the acceptor Tc in above three doped crystals are 10.01 ns, 14.51 ns and 2.37 ns, respectively. As can be seen, the decay time of Tc in the DSB<Tc-Pc crystal has a large decrease to 2.37 ns compared with that in the DSB<Tc crystals, indicating the energy transfer efficiently from Tc to Pc in the white-emissive doubly doped crystal. Figure 3c shows the photoluminescence decay curves of DSB<Pc crystals with two different mol ratios (DSB: Pc = 28: 1, 16: 1), and the white-emissive doubly doped DSB<Tc-Pc crystal (DSB: Tc: Pc = 20: 1: 0.9) monitored at the emission wavelength of 608 nm. The decay time of the acceptor Pc in above three doped crystals are 6.92 ns, 8.29 ns and 8.06 ns, respectively. This indicates the decay time of Pc in the doped crystals is proportional to its doping concentration and the acceptor molecules are embedded in the DSB crystal with approximately uniform dispersion. A summary of transient photoluminescence decay time for the above systems is given in Table 2. The emission properties of DSB<Tc (DSB: Tc = 33: 1, 18: 1) and DSB<Pc (DSB: Pc = 28: 1, 16: 1) crystals are given in the supporting information.

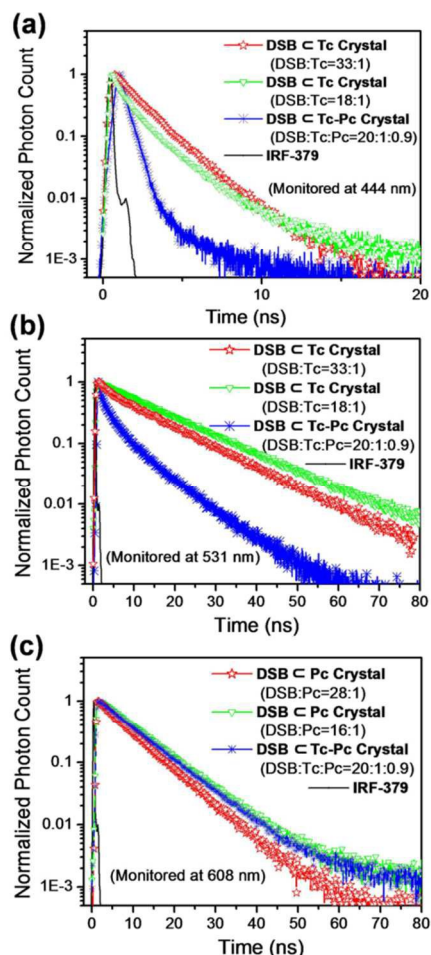


**Fig. 3** Time-resolved fluorescence decay curves of the white-emissive doubly doped DSB<Tc-Pc crystal (DSB: Tc: Pc = 20: 1: 0.9) monitored at different emission wavelengths. The decay curves of DSB<Tc crystals (DSB: Tc = 33: 1, 18: 1) and DSB<Pc crystals (DSB: Pc = 28: 1, 16: 1) with different mol ratios are also given for comparison. (a)  $\lambda_{em}$  = 444 nm; (b)  $\lambda_{em}$  = 531 nm; (c)  $\lambda_{em}$  = 608 nm.

**Table 2** Decay data of the white-emissive doubly doped DSB<Tc-Pc crystal (DSB: Tc: Pc = 20: 1: 0.9), DSB<Tc crystals (DSB: Tc = 33: 1, 18: 1) and DSB<Pc crystals (DSB: Pc = 28: 1, 16: 1) with different mol ratios monitored at the emission wavelengths of 444 nm, 531 nm and 608 nm, respectively.

Crystal	Decay time $\tau$ (ns)	Percentage (%)	Mean lifetime $\tau$ (ns)	$\lambda_{em}$ (nm)
DSB<Tc crystal (DSB: Tc= 33: 1)	2.28 1.04	36.09 63.91	1.49	444
DSB<Tc crystal (DSB: Tc= 18: 1)	1.94 0.50	34.47 65.20	1.04	
DSB<Tc-Pc crystal (DSB: Tc: Pc = 20: 1: 0.9)	0.79 0.09	2.67 97.33	0.11	
DSB<Tc crystal (DSB: Tc= 33: 1)	13.23 2.110	71.07 28.93	10.01	531
DSB<Tc crystal (DSB: Tc= 18: 1)	14.51	100	14.51	
DSB<Tc-Pc crystal (DSB: Tc: Pc = 20: 1: 0.9)	7.30 0.86	23.39 76.61	2.37	
DSB<Pc crystal (DSB: Pc= 28: 1)	6.92	100	6.92	608
DSB<Pc crystal (DSB: Pc= 16: 1)	8.29	100	8.29	
DSB<Tc-Pc crystal (DSB: Tc: Pc = 20: 1: 0.9)	8.06	100	8.06	

Based on the above analyses, it is demonstrated that the energy transfer occurs not only from the donor DSB to the acceptors Tc and Pc but also from the acceptor Tc to the acceptor Pc in the white-emissive doubly doped DSB<Tc-Pc crystal. Herein, it is much worthy of attention to the stacking mode between molecules which decides the host-guest intermolecular dipole orientation impacting on the energy transfer process in the DSB<Tc-Pc crystal.

### 3. Morphology and structure of the white-emissive DSB<Tc-Pc crystal

Figure 4a shows the AFM height image at the surface areas of the DSB<Tc-Pc crystal (DSB: Tc: Pc = 20: 1: 0.9). Step-like morphology has been found. From the cross-section analyses, the average height of steps observed on the crystal surface is about 1.78 nm. Figure 4b shows the diffraction patterns of wide-angle X-ray diffraction (XRD) on the above mentioned slice doped crystal and comparatively pure DSB crystal. As can be seen, the diffraction peaks occur equidistantly with angle degree varying, and the diffraction peaks are very sharp, so the doped crystal

should have the good ordered layer structures. The lattice parameters of pure DSB were reported by Wu et al.<sup>25</sup>  $a=5.87$  Å,  $b=7.70$  Å,  $c=34.87$  Å. Possible herringbone arrangement of DSB molecules in crystal was recognized in previous work.<sup>38,39</sup>

According to the Bragg equation  $2dsin\theta = n\lambda$ , the thickness of one molecular layer of DSBcTc-Pc crystal is calculated to be 1.76 nm, which corresponds to the one-step height of the doped crystal in AFM image.

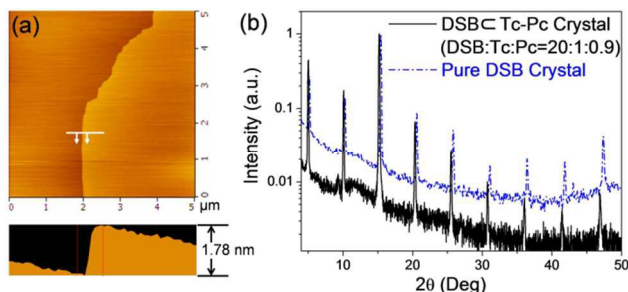


**Fig. 4** (a) AFM height image of the surface of DSBcTc-Pc crystal (DSB: Tc: Pc= 20: 1: 0.9) and its enlarged sectional analysis. (b) Wide-angle X-ray diffraction patterns of DSBcTc-Pc crystal (DSB: Tc: Pc= 20: 1: 0.9) and pure DSB crystal.

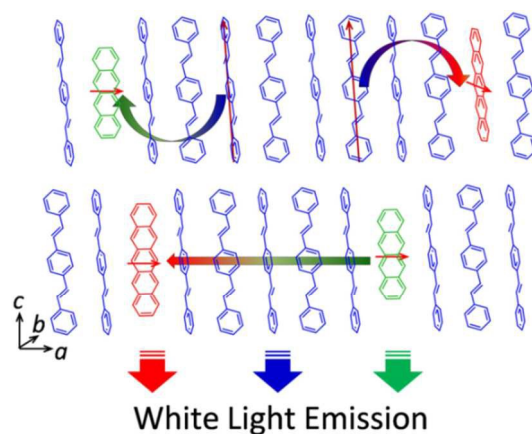
The results of AFM morphology and X-ray diffraction pattern suggest that the DSBcTc-Pc crystal has the layer-by-layer structure and each layer corresponds to a molecular monolayer. So the structural ordering of the DSBcTc-Pc crystal has been retained after doping a certain quantity of Tc and Pc molecules into the DSB matrix, which means doped guest molecules may replace the locations of original host molecules in the crystal lattice. Doping Tc and Pc into DSB crystal leads the layer space to a little larger (one molecular layer thickness of pure DSB crystal is 1.72 nm), attributed to the disturbance of the intrinsic DSB crystal lattices caused by the embedment of doped molecules. Importantly, both DSB as the host molecules and Tc/Pc as the guest molecules are all the linear configurations and the molecules in the crystals are arranged in similar 'herringbone' type structure in the  $ab$  plane, where edge-to-face arene-arene interactions are much stronger than intermolecular interactions along the  $c$  axis direction; thus, the cross transition dipole arrangement between DSB and Tc/Pc molecules is fixed when the layer-by-layer structure is formed.

Figure 5 shows the schematics of the proposed molecular stacking and energy transfer process in the white-emissive DSBcTc-Pc crystal. The energy is usually considered to transfer along the direction of molecular transition dipole from donor to acceptor. When RET is 50% efficient, the donor-acceptor distance is equal to the Förster distance  $R_0$ ,<sup>40</sup> which could be described as follows:

$$R_0^6 = \frac{9000(\ln 10)\kappa^2\phi_D}{128\pi^5 n^4 N_A} J_C$$

where  $\phi_D$  is the quantum yield of the donor in the absence of acceptor,  $n$  is the refractive index of the medium,  $N_A$  is Avogadro's number,  $J_C$  is the spectral overlap integral calculated as  $J_C = \int_0^\infty F_D(\lambda)\epsilon_A(\lambda)\lambda^4 d\lambda$ .  $F_D(\lambda)$  is the normalized donor emission spectrum, and  $\epsilon_A(\lambda)$  is the acceptor molar extinction coefficient. Notably, as mentioned in above equation, the Förster

distance  $R_0$  is in direct proportional to the orientation factor  $\kappa^2$  when the donor-acceptor species are confirmed, which means the spatial orientation of the donor and acceptor molecular transition dipoles determines the energy transfer efficiency. Therefore, the almost mutually perpendicular dipole orientation between DSB and Tc/Pc should be not conducive to energy transfer which  $\kappa^2$  could be estimated to be 0.004–0.008 as proved in our previous work;<sup>28</sup> but head-to-tail dipole orientation should be conducive to energy transfer that occurs between Tc and Pc in the white-emissive DSBcTc-Pc crystal. It is also the reason that the doping concentration of Tc and Pc is approximately 10% (equivalent to shorten the donor-acceptor distance) and the relatively efficient energy transfer between hosts and guests can be achieved, which is attributed to the cross donor-acceptor transition dipole arrangement.



**Fig. 5** Proposed molecular stacking of the doubly doped DSBcTc-Pc crystal. The energy transfer processes in the white-light-emission crystal are illustrated by the colorful arrows.

#### 4. Field-effect mobility measurement of white-emissive DSBcTc-Pc crystal

The hole- and electron-transport FETs based on the white-emissive DSBcTc-Pc crystal were constructed, respectively. Gold and calcium electrodes were chosen for the hole- and electron-carrier injections, considering the host DSB HOMO and LUMO levels of  $\sim 5.3$  eV and  $\sim 2.3$  eV, respectively. Figure 6 shows the output and transfer characteristics of top-contact p- and n-type OFETs based on white-emissive DSBcTc-Pc crystals. Both p- and n-type FET operation was clearly observed under applied negative and positive  $V_{GS}$  with a saturated hole mobility of  $\mu_h = 1.62 \times 10^{-2}$  cm<sup>2</sup>/Vs and a saturated electron mobility of  $\mu_e = 2.15 \times 10^{-4}$  cm<sup>2</sup>/Vs. As comparison, the pure DSB crystal-based FET was constructed and the hole mobility was measured with  $\sim 0.02$  cm<sup>2</sup>/Vs (see Figure S4 in the supporting information), which indicates the structural ordering maintenance of the white-emissive DSBcTc-Pc crystal could ensure the hole carrier mobility comparable to that of undoped host. Meanwhile, the electron mobility was two orders of magnitude lower than the hole mobility in the DSBcTc-Pc crystal because the LUMO level of DSB ( $\sim 2.3$  eV) and the work function (WF) of calcium ( $\sim 2.9$  eV) was not well aligned resulting to the electron-injection difficulty. The non-balanced transport of hole- and electron-carriers is unfavourable to realize a white electroluminescence of DSBcTc-Pc crystal using the light-emitting FET devices.

Therefore, the novel host crystalline material with the energy levels matching to the electrode WF suitable for the white-emissive doped organic crystal growth is going to be investigated.

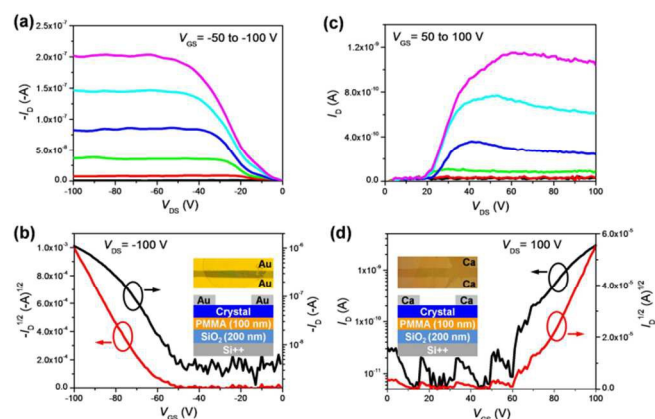


**Fig. 6** Output characteristics (a, c) and transfer characteristics (b, d) of OFETs based on white-emissive DSBcTc-Pc crystals with symmetric gold and calcium electrodes, respectively. The inserts in figure (b, d) are the device configurations and their top-view photographs. Channel length ( $L$ ) and width ( $W$ ) were determined by optical microscopy:  $L/W=100/1050\ \mu\text{m}$  (b);  $L/W=100/340\ \mu\text{m}$  (d).

### 5. The chromaticity-stable white-emissive DSBcTc-Pc crystal

The stability of the crystal is considered to be an inherent characteristic due to the highly ordered and tight arrangement between molecules. For the white-emissive DSBcTc-Pc crystal with the determined mol ratio of host to guest molecules, the intermolecular edge-to-face arene-arene interactions between DSB and Tc/Pc would immobilize their spatial orientations of transition dipoles which contribute to retain the color stability even in the conditions of high-density photons excitation or charges injection. To verify the color stability of the white-emissive DSBcTc-Pc crystal, the photoluminescence properties of the crystal excited with different pumping laser energy have been implemented. The crystal adhered to the quartz substrate was irradiated by the third harmonic (355 nm) of a Nd:YAG (yttrium-aluminum-garnet) laser in the experiment (Figure 7c shows the crystal photograph under the laser excitation); and the emission spectra were detected by a CCD fiber spectrograph. With the increase of pumping laser energy, the photoluminescence intensity of the white-emissive DSBcTc-Pc crystal will also increase as shown in Figure 7a. The crystal emission exhibits the good color stability with the CIE coordinates from (0.37, 0.39) to (0.32, 0.35) in Figure 7b as the pumping laser energy varying from 45 to 1900 KW/cm<sup>2</sup>; as comparison a doubly doped DSBcTc-Pc thin film (DSB: Tc: Pc=300: 1: 1) with the 300 nm thickness was prepared by the vacuum deposition and the thin film emission spectra present a distinct variation with the pumping laser energy increasing from 12 to 60 KW/cm<sup>2</sup>, which may be due to the molecular aggregate state change from amorphous to crystalline in the doped thin film induced by the thermal effect of higher laser energy radiation. The emission spectra data of the DSBcTc-Pc thin film is given in the supporting information. Therefore, the doped organic crystal has the high potential of realizing a stable white electroluminescence towards organic light-emitting devices.

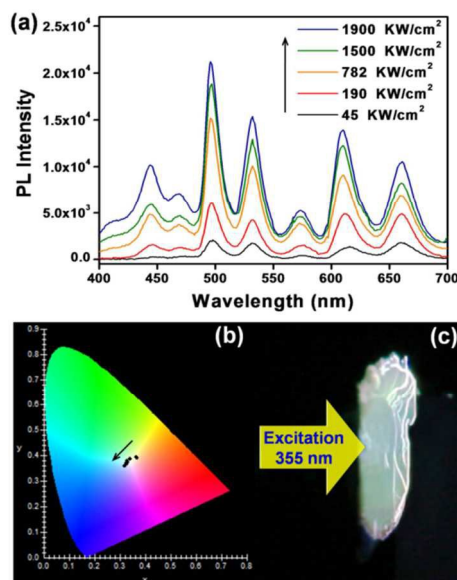


**Fig. 7** (a) Photoluminescence spectra of the white-emissive DSBcTc-Pc crystal as the variation of the pumping laser energy. (b) CIE chromaticity diagram marked with the coordinates of (0.37, 0.39), (0.35, 0.38), (0.34, 0.37), (0.33, 0.36) and (0.32, 0.35) corresponding to the crystal emissions excited with the pumping laser energy of 45, 190, 782, 1500 and 1900 KW/cm<sup>2</sup> respectively in Figure 7a. (c) The optical photograph of the white-emissive DSBcTc-Pc crystal excited with 355 nm pumping laser.

### Conclusions

Large-size and stable white-emissive DSBcTc-Pc crystal with the specific mol ratio of host to guest molecules (DSB: Tc: Pc = 20: 1: 0.9) has been prepared by PVT method. The results of time-resolved fluorescence indicate that the energy transfer occurs not only from the donor DSB to the acceptors Tc and Pc but also from the acceptor Tc to the acceptor Pc in the DSBcTc-Pc crystal. The host DSB matrix with the embedment of a certain quantities of Tc and Pc molecules retains the structural ordering verified by AFM and XRD, which benefits for the carrier transport; and the hole and electron field-effect mobility of the DSBcTc-Pc crystal can be up to  $1.62 \times 10^{-2}\ \text{cm}^2/\text{Vs}$  and  $2.15 \times 10^{-4}\ \text{cm}^2/\text{Vs}$ , respectively. Compared with the amorphous DSBcTc-Pc film, the crystal emission exhibits the better color stability even under the high pumping laser energy excitation. Further developing the well-balanced carrier-transport doped organic crystal with high mobility would be promising to realize a stable organic white lighting crystal device.

### Acknowledgements

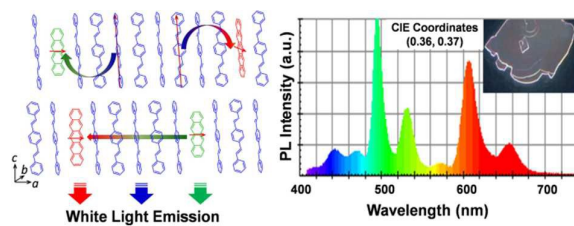
We are grateful for financial support from the Youth Science Foundation of Heilongjiang Province (QC2014C046), Open Project of State Key Laboratory of Supramolecular Structure and Materials (Grant Number sklssm201428).

### Notes and references

- <sup>a</sup> College of Chemistry and Chemical Engineering, Northeast Petroleum University, Daqing, 163318, PR China. Fax: (+86)459-6504154; Tel: (+86)459-6504154; E-mail: wanghuan83214@gmail.com  
<sup>b</sup> State Key Laboratory of Luminescent Materials and Devices, Institute of Polymer Optoelectronic Materials and Devices, South China University

- of Technology, Guangzhou, 510640, PR China. E-mail: yigma@scut.edu.cn
- <sup>c</sup> Department of Physics, Graduate School of Science, Tohoku University, Sendai, 980-8578, Japan. E-mail: shanghai0625@gmail.com
- <sup>d</sup> State Key Laboratory of Supramolecular Structure and Materials, Jilin University, Changchun, 130012, PR China.
- † Electronic Supplementary Information (ESI) available: The details of chromatograph analysis to the white-emissive DSBcTc-Pc crystal, the emission spectra of singly doped crystals, the data of pure DSB crystal-based field-effect transistors and the color stability test of the doped thin film excited with different pumping laser energy. See DOI: 10.1039/b000000x/
- 1 M. Pope, H. P. Kallmann and P. Mangnante, *J. Chem. Phys.*, 1963, **38**, 2042.
  - 2 O. S. Avanesjan, V. A. Benderskii, V. K. Brikenstein, V. L. Broude, L. I. Korshunov, A. G. Lavrushko and I. I. Tartakovskii, *Mol. Cryst. Liq. Cryst.*, 1974, **29**, 165.
  - 3 D. Fichou, S. Delysee and J. M. Nunzi, *Adv. Mater.*, 1997, **9**, 1178.
  - 4 V. Y. Butko, X. Chi and A. P. Ramirez, *Solid State Commun.*, 2003, **128**, 431.
  - 5 A. Dadvand, A. G. Moiseev, K. Sawabe, W. H. Sun, B. Djukic, I. Chung, T. Takenobu, F. Rosei and D. F. Perepichka, *Angew. Chem. Int. Ed.*, 2012, **51**, 3837.
  - 6 Z. Q. Xie, B. Yang, F. Li, G. Cheng, L. L. Liu, G. D. Yang, H. Xu, L. Ye, M. Hanif, S. Y. Liu, D. G. Ma and Y. G. Ma, *J. Am. Chem. Soc.*, 2005, **127**, 14152.
  - 7 H. Yanagi, T. Ohara and T. Morikawa, *Adv. Mater.*, 2001, **13**, 1452.
  - 8 M. Ichikawa, R. Hibino, M. Inoue, T. Haritani, S. Hotta, T. Koyama and Y. Taniguchi, *Adv. Mater.*, 2003, **15**, 213.
  - 9 S. Varghese, S. J. Yoon, S. Casado, R. C. Fischer, R. Wannemacher, S. Y. Park and J. Gierschner, *Adv. Optical Mater.*, 2014, **2**, 542.
  - 10 V. C. Sundar, J. Zaumseil, V. Podzorov, E. Menard, R. L. Willett, T. Someya, M. E. Gershenson and J. A. Rogers, *Science*, 2004, **303**, 1644.
  - 11 A. L. Briseno, S. C. B. Mannsfeld, M. M. Ling, S. Liu, R. J. Tseng, C. Reese, M. E. Roberts, Y. Yang, F. Wudl and Z. N. Bao, *Nature*, 2006, **444**, 913.
  - 12 T. He, M. Stolte and F. Würthner, *Adv. Mater.*, 2013, **25**, 6951.
  - 13 X. J. Li, Y. X. Xu, F. Li and Y. G. Ma, *Org. Electron.*, 2012, **13**, 762.
  - 14 S. Z. Bisri, T. Takenobu, Y. Yomogida, H. Shimotani, T. Yamao, S. Hotta and Y. Iwasa, *Adv. Funct. Mater.*, 2009, **19**, 1728.
  - 15 T. Komori, H. Nakanotani, T. Yasuda and C. Adachi, *J. Mater. Chem. C*, 2014, **2**, 4918.
  - 16 R. J. Tseng, R. Chan, V. C. Tung and Y. Yang, *Adv. Mater.*, 2008, **20**, 435.
  - 17 Y. J. Zhang, H. L. Dong, Q. X. Tang, S. Ferdous, F. Liu, S. C. B. Mannsfeld, W. P. Hu and A. L. Briseno, *J. Am. Chem. Soc.*, 2010, **132**, 11580.
  - 18 Q. H. Cui, L. Jiang, C. Zhang, Y. S. Zhao, W. P. Hu and J. N. Yao, *Adv. Mater.*, 2012, **24**, 2332.
  - 19 Y. V. Naboikin, L. A. Ogurtsova, A. P. Podgorny and L. Y. Malkes, *SOV. J. QUANTUM ELECTRON.*, 1978, **8**, 457.
  - 20 H. S. Avanesyan, V. A. Benderskii, V. K. Brikenstein, A. G. Lavrushko and P. G. Filippov, *phys. stat. sol. (a)*, 1975, **30**, 781.
  - 21 Y. S. Zhao, H. B. Fu, F. Q. Hu, A. D. Peng, W. S. Yang and J. N. Yao, *Adv. Mater.*, 2008, **20**, 79.
  - 22 T. Takenobu, S. Z. Bisri, T. Takahashi, M. Yahiro, C. Adachi and Y. Iwasa, *Phys. Rev. Lett.*, 2008, **100**, 066601.
  - 23 K. Sawabe, M. Imakawa, M. Nakano, T. Yamao, S. Hotta, Y. Iwasa and T. Takenobu, *Adv. Mater.*, 2012, **24**, 6141.
  - 24 H. Wang, F. Li, B. R. Gao, Z. Q. Xie, S. J. Liu, C. L. Wang, D. H. Hu, F. Z. Shen, Y. X. Xu, H. Shang, Q. D. Chen, Y. G. Ma and H. B. Sun, *Cryst. Growth Des.*, 2009, **9**, 4945.
  - 25 C. C. Wu, M. C. Delong, Z. V. Vardeny and J. P. Ferraris, *Synth. Met.*, 2003, **137**, 939.
  - 26 H. M. Cuppen, W. S. Graswinckel and H. Meeke, *Cryst. Growth Des.*, 2004, **4**, 1351.
  - 27 R. Ruiz, D. Choudhary, B. Nickel, T. Toccoli, K. C. Chang, A. C. Mayer, P. Clancy, J. M. Blakely, R. L. Headrick, S. Iannotta and G. G. Malliaras, *Chem. Mater.*, 2004, **16**, 4497.
  - 28 H. Wang, B. L. Yue, Z. Q. Xie, B. R. Gao, Y. X. Xu, L. L. Liu, H. B. Sun and Y. G. Ma, *Phys. Chem. Chem. Phys.*, 2013, **15**, 3527.
  - 29 H. Wang, Y. Zhao, Z. Q. Xie, H. Y. Wang, B. H. Wang and Y. G. Ma, *CrystEngComm*, 2014, **16**, 4539.
  - 30 Z. Q. Xie, W. J. Xie, F. Li, L. L. Liu, H. Wang and Y. G. Ma, *J. Phys. Chem. C*, 2008, **112**, 9066.
  - 31 T. Förster, *Discuss. Faraday Soc.*, 1959, **27**, 7.
  - 32 J. Gierschner, L. Lüer, B. M. n-Medina, D. Oelkrug and H. -J. Egelhaaf, *J. Phys. Chem. Lett.*, 2013, **4**, 2686.
  - 33 J. M. Robertson, V. C. Sinclair and J. Trotter, *Acta Cryst.*, 1961, **14**, 697.
  - 34 R. B. Campbell, J. M. Robertson and J. Trotter, *Acta Crystallogr.*, 1962, **15**, 289.
  - 35 S. H. Lim, T. G. Bjorklund, F. C. Spano and C. J. Bardeen, *Phys. Rev. Lett.*, 2004, **92**, 107402.
  - 36 H. B. Klevens and J. R. Platt, *J. Chem. Phys.*, 1949, **17**, 470.
  - 37 H. Wang, Z. Q. Xie, B. Yang, F. Z. Shen, Y. P. Li and Y. G. Ma, *CrystEngComm*, 2008, **10**, 1252.
  - 38 F. C. Spano, *Ann. Rev. Phys. Chem.*, 2006, **57**, 217.
  - 39 J. Gierschner, M. Ehni, H. -J. Egelhaaf, B. Milián Medina, D. Beljonne, H. Benmansour and G. C. Bazan, *J. Chem. Phys.*, 2005, **123**, 144914.
  - 40 T. Förster, *Ann. Phys.*, 1948, **2**, 55.

### The table of contents entry



The structural, optical and charge-transport properties of a white-emissive doped organic crystal have been investigated.